Title
Improving a high-efficiency, gated spectrometer for x-ray Thomson scattering experiments at the National Ignition Facility.

Journal
The Review of scientific instruments, 87(11)

ISSN
0034-6748

Authors
Döppner, T
Kraus, D
Neumayer, P
et al.

Publication Date
2016-11-01

DOI
10.1063/1.4959874

Peer reviewed

AIP | Review of Scientific Instruments

Improving a high-efficiency, gated spectrometer for x-ray Thomson scattering experiments at the National Ignition Facility

T. Döppner, D. Kraus, P. Neumayer, B. Bachmann, J. Emig, R. W. Falcone, L. B. Fletcher, M. Hardy, D. H. Kalantar, A. L. Kritcher, O. L. Landen, T. Ma, A. M. Saunders, and R. D. Wood

Citation: Review of Scientific Instruments **87**, 11E515 (2016); doi: 10.1063/1.4959874
View online: http://dx.doi.org/10.1063/1.4959874
View Table of Contents: http://scitation.aip.org/content/aip/journal/rsi/87/11?ver=pdfcov
Published by the AIP Publishing

Improving a high-efficiency, gated spectrometer for x-ray Thomson scattering experiments at the National Ignition Facility

T. Döppner,[1,a)] D. Kraus,[2] P. Neumayer,[3] B. Bachmann,[1] J. Emig,[1] R. W. Falcone,[2,4] L. B. Fletcher,[5] M. Hardy,[1] D. H. Kalantar,[1] A. L. Kritcher,[1] O. L. Landen,[1] T. Ma,[1] A. M. Saunders,[2] and R. D. Wood[1]

[1]*Lawrence Livermore National Laboratory, Livermore, California 94720, USA*
[2]*University of California, Berkeley, California 94720, USA*
[3]*Gesellschaft für Schwerionenphysik, Darmstadt, Germany*
[4]*Lawrence Berkeley National Laboratory, Berkeley, California 94720, USA*
[5]*SLAC National Accelerator Laboratory, Menlo Park, California 94720, USA*

(Presented 8 June 2016; received 9 June 2016; accepted 29 June 2016; published online 3 August 2016)

We are developing x-ray Thomson scattering for applications in implosion experiments at the National Ignition Facility. In particular we have designed and fielded MACS, a high-efficiency, gated x-ray spectrometer at 7.5–10 keV [T. Döppner *et al.*, Rev. Sci. Instrum. **85**, 11D617 (2014)]. Here we report on two new Bragg crystals based on Highly Oriented Pyrolytic Graphite (HOPG), a flat crystal and a dual-section cylindrically curved crystal. We have performed *in situ* calibration measurements using a brass foil target, and we used the flat HOPG crystal to measure Mo K-shell emission at 18 keV in 2nd order diffraction. Such high photon energy line emission will be required to penetrate and probe ultra-high-density plasmas or plasmas of mid-Z elements. *Published by AIP Publishing.* [http://dx.doi.org/10.1063/1.4959874]

I. INTRODUCTION

Accurate characterization of warm and hot dense matter is important for modeling high energy density physics experiments that aim, for example, at advancing our understanding of inertial confinement fusion[1] and astrophysical objects.[2] X–ray Thomson scattering (XRTS) is a powerful *in situ* plasma diagnostic since it uses high energy x rays that are able to penetrate dense and compressed matter, and allows to infer key plasma parameters like temperature, density, ionization, and structure factors.[3,4] We are developing XRTS for spherical implosion experiments at the National Ignition Facility (NIF).[5–9] In this paper we focus on reporting on further improvements to the Mono Angle Crystal Spectrometer (MACS), which is a high-collection efficiency, gated x-ray spectrometer for XRTS with Zn He_α line emission at 9 keV at the NIF.[7] The initial MACS design used a cylindrically curved HOPG (highly oriented pyrolytic graphite) crystal, which focuses the x-rays in the non-dispersive axis. This provides high collection efficiency and crude spatial resolution along the non-dispersive axis, which enables spatial discrimination of possible background signals. The downside of this approach is that only one spectrum per experiment can be recorded. Recently we implemented a more rigorous shielding design at the target that successfully blocks the line of sight to the MACS spectrometer for relevant background signals.[6] This opens new options for x-ray crystals since the requirements for spatial resolution of the spectrometer can be relaxed. We have designed and fielded two additional new HOPG crystals for MACS, a flat crystal and a dual-section cylindrical crystal. In this paper we will discuss the design of these crystals and calibration measurements.

II. NEW CRYSTAL OPTIONS FOR MACS

Fig. 1 describes the setup for the dual-section cylindrical crystal. It consists of two cylindrical surfaces side by side, which are 15 mm wide each. The valleys of these cylinders are placed such that they are on a straight line for the 8.6 keV reflection off the center of the crystal between the x-ray emission source and strip 1 and strip 3, respectively, of a 4-strip microchannel plate (MCP) detector (see Fig. 1(a)). Since the MCP strips are 9.5 mm apart, and the spectrometer operates at a magnification of one, this requires a separation of the valleys of 9.5 mm. Thus each cylinder section is slightly asymmetric, where the valley is located 4.75 mm sideways from the center of the combined crystal. This fact is further illustrated by the relative height map in Fig. 1(b). The dispersion of the spectrometer is set by the direct distance of the x-ray source to the detector (490 mm) and the normal distance of this direct line to the bottom of the cylinders (see Fig. 1(a) in Ref. 7). In order to maintain the same dispersion across different crystals, the absolute height in the dual cylinder crystal surface is set such that the valleys are at the same normal distance to the symmetry line (source to detector) of 54 mm as in the single cylinder case.[7] Fig. 1(b) shows a CAD drawing of the crystal substrate. In addition to the crystal surface, it shows the four holes for mounting the crystal to the spectrometer body and the curvature of the outside surface, which is designed to minimize interference with neighboring laser beams. The substrate is

Note: Contributed paper, published as part of the Proceedings of the 21st Topical Conference on High-Temperature Plasma Diagnostics, Madison, Wisconsin, USA, June 2016.
[a)]Author to whom correspondence should be addressed. Electronic mail: doeppner1@llnl.gov.

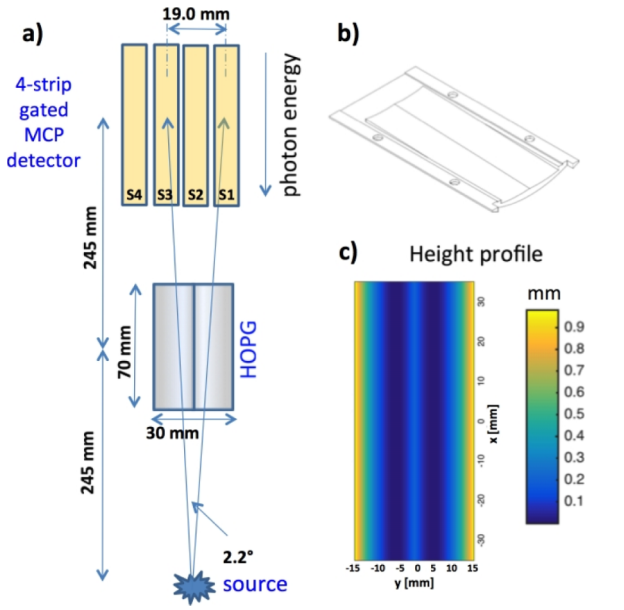

FIG. 1. (a) Schematic geometry of the dual-section cylindrically curved crystal for MACS, which focuses x-rays onto strip one and three of a 4-strip gated x-ray detector. (b) CAD model of the Al substrate. (c) Height map of the dual-section cylindrically curved crystal surface. The valleys of the crystal are separated by 9.5 mm, spanning a divergence angle of 2.2°.

made out of aluminum (Al 6061-T6). The crystal surface is cut with a radius of curvature of 54 mm by a diamond turning machine maintaining a profile tolerance of 5 μm. In order to achieve high collection efficiency, we use HOPG as the Bragg crystal, which has the highest known integrated reflectivity, R_{int}, of 5 mrad at 9 keV.[10,11] A 300 μm thick HOPG coating layer was applied by Optigraph (Berlin, Germany). A ~10 μm thick layer of glue was used to avoid delamination in vacuum. The mosaicity of the crystal is quoted to meet $\gamma \leq 0.8°$, however, the focusing characteristics indicate that it could be as high as $\gamma = 1.3°$ (Ref. 7 and Fig. 2).

The design of the new flat HOPG crystal is conceptually much simpler. The 30 mm × 70 mm, 2 mm thick crystals were procured from Momentive Performance Materials (Strongsville, USA), and are quoted to have ZYB quality, i.e., the crystal mosaicity meets $\gamma \leq 0.8°$. Analyzing the shadow of a sharp edge to 9 keV x-rays we measure $\gamma = 0.55°$. The general crystal substrate layout is similar to the one shown in Fig. 1(b). As discussed above, to maintain the same spectral dispersion we recessed the substrate surface by 1.7 mm

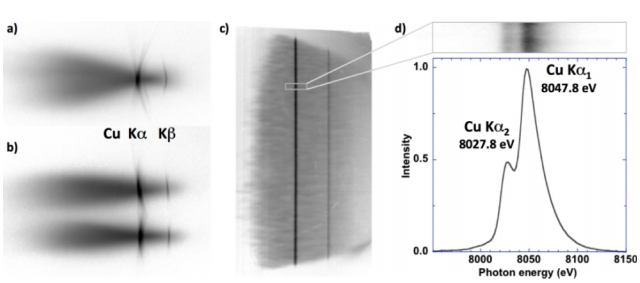

FIG. 2. Calibration measurements with a Manson source of (a) a single cylindrically curved, (b) a dual cylinder, and (c) a flat HOPG crystal. The latter provides a spectral resolution of better than 20 eV at 8.0 keV (d).

compared to the valley heights of the cylindrical crystals to account for the difference in flat crystal thickness compared to the HOPG coatings.

III. CALIBRATION MEASUREMENTS

We have done a number of performance qualification measurements, which are summarized in this section. First, we used a Manson source to measure the reflection homogeneity and confirm the focusing concept of the dual cylinder crystal. The source consisted of a copper anode operated at an accelerating voltage of 10.0 kV, which is above the K-shell ionization threshold for copper. The crystal and the detector were arranged to match the MACS spectrometer geometry, i.e., the crystals were placed at a distance of 250 mm from the x-ray source. The x-ray spectra were recorded with an image plate detector (Fujifilm SR),[12] and scanned within 30 min of exposure. Typical exposure times ranged from 1 min for the singly curved crystal to 10 min for the flat crystal.

The results of these measurements are summarized in Fig. 2. The image data clearly show the copper line emission ($K_{\alpha 2}$: 8027.8 eV, $K_{\alpha 1}$: 8047.8 eV, K_{β}: 8905.3 eV) on top of the continuum emission. The data are presented on a logarithmic grey scale to make the continuum contribution more visible, which highlights the focusing properties of the curved crystals (Figs. 2(a) and 2(b)). Note that the reduced divergence of the spectrum at lower energies for the dual-section crystal is consistent with the two times lower f-number of the individual crystals. In our NIF scattering experiments[5,6,9] lineouts are taken over a 2 mm high box near the focus of the crystals; therefore the off-axis low-intensity aberrations do not have an impact on the spectral resolution of those measurements. The flat crystal (Fig. 2(c)) shows excellent homogeneity in the reflection across the crystal, and yields highly resolved spectral lines. Fig. 2(d) shows a lineout across the copper K_{α} lines, which can clearly be resolved.

The dispersion of all crystals was measured in-situ in the NIF target chamber by recording Cu and Zn K-shell line emission from a brass foil target. In these measurements the MACS spectrometers are looking at the foils under a small glancing angle to reduce the source size to 200 μm in the dispersive direction.[7] Compared to Ref. 7 we reduced the Al filtering in front of the MCP detector from 900 to 600 μm to enhance the line emission over the high-energy continuum background that is reflected in second diffraction order. Table I summarizes the MACS calibration measurements with HOPG in first order that have been conducted to date. These measurements find the dispersion at 9.0 keV for the various

TABLE I. Calibration measurements for MACS crystals.

Shot	Diagnostic port	Crystal	Dispersion at 9 keV (eV/mm)
N130322-001-999	0-0	Singly curved	83.1
N150323-002-999	90-78	Singly curved	84.0
	0-0	Flat	83.1
N150621-001-999	90-78	Dual curved	83.4

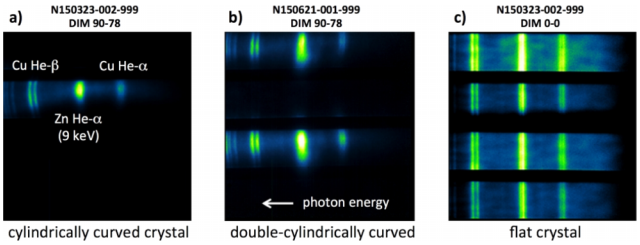

FIG. 3. Gallery of calibration measurements from laser-heated brass foils for each of the HOPG crystals qualified to date. For details see text.

crystals to be within ±0.5% of the nominal dispersion, which successfully confirms the crystal design approach discussed above and the manufacturing to tolerances. Fig. 3 shows a gallery of calibration data taken for each of the different crystal designs. It illustrates the trade-off between the number of MCP strips illuminated (which determines the number of probing times for a given experiment) and the signal collected in a given spectrum. Taking into account the detector gain changes, the signal levels are consistent with the HOPG widths that the x rays are reflecting off, which are 30, 15, and 3.75 mm for the singly and doubly curved and the flat crystals, respectively. For ongoing NIF scattering experiments,[6] it turns out that the dual-section curved crystal is an excellent compromise between high signal collection, achieving time resolution, and maintaining imaging capabilities in the non-dispersive direction to identify the source of potential background signals.

IV. SPECTRA IN SECOND DIFFRACTION ORDER

We have started to characterize the flat HOPG crystals in second diffraction order, for which we expect R_{int} = 0.75 mrad.[11] On NIF shot N150621-001-999 we heated a 25 μm thick Mo foil with two laser quads (Q46B and Q46T) focused to 150 μm spot size. The laser delivered a total of 38.0 kJ at 355 nm onto the foil. Peak intensity of I_p = 1.0 × 10^{17} W/cm^2 was reached 4.0 ns after a picket at 0.11× I_p. To suppress x-ray emission in first order the detector was filtered with a total of 425 μm Ti. It shows a single feature near 18 keV, see Fig. 4, where the line to continuum ratio is about seven. Spectral lineouts are shown in comparison to a similar foil shot on Omega,[4] which used the same laser intensity, but had a reduced prepulse delay (1 ns) and a smaller spot size (80 μm). Two clear differences in the experimental data stand out: (1) The NIF spectrum is more narrow (470 eV vs. 600 eV FWHM) and (2) the NIF spectrum has an additional tail at high energies. The latter is due to depth-broadening, which is caused by reflections deep inside the 2 mm thick crystal.[11] It is absent in the Omega data, which were taken with a thinner (d = 300 μm) crystal. A FWHM of 310 eV of the Mo He$_\alpha$ lines at 17.907 and 18.062 keV and taking into account the effect of depth broadening yields a good fit of the NIF data.

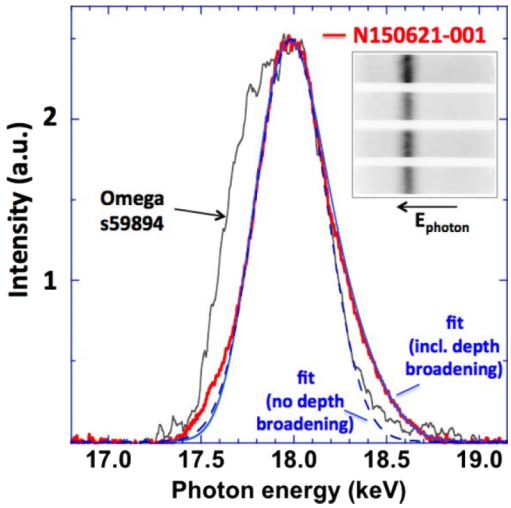

FIG. 4. NIF molybdenum foil emission spectrum in comparison to Omega measurement. The NIF data can be fitted assuming emission at Mo He$_\alpha$ lines and depth broadening by the 2 mm thick HOPG crystal.

The additional red-shifted component in the Omega data is likely due to incomplete ionization to the He–like state despite the same laser drive intensity. However, due to the smaller focal spot size at Omega the fraction of cooler plasma in the peripheral zone of the laser spot is larger than in the NIF case. The demonstration of Mo He$_\alpha$ emission with reduced spectral width shows promise for future XRTS measurements of plasmas at extreme densities ($n_e \sim 10^{25}$ cm^{-3}) and of mid-Z elements at the NIF.

ACKNOWLEDGMENTS

We thank Vladimir Arkadiev, Herbert Legall and Inna Grigorieva of Optigraph GmbH, Berlin, for many helpful discussions on graphite coatings. This work was performed under the auspices of the U.S. Department of Energy by the Lawrence Livermore National Laboratory under contract DE-AC52-07NA27344. The authors acknowledge support from Laboratory Directed Research and Development Grant No. 13-ERD-073.

[1]J. D. Lindl *et al.*, Phys. Plasmas **11**, 339 (2004).
[2]L. Stixrude, Phys. Rev. Lett. **108**, 055505 (2012).
[3]S. H. Glenzer and R. Redmer, Rev. Mod. Phys. **181**, 1625 (2009).
[4]T. Ma *et al.*, Phys. Plasmas **21**, 056302 (2014).
[5]T. Döppner *et al.*, J. Phys.: Conf. Ser. **500**, 192019 (2014).
[6]D. Kraus *et al.*, J. Phys.: Conf. Ser. **717**, 012067 (2016).
[7]T. Döppner *et al.*, Rev. Sci. Instrum. **85**, 11D617 (2014).
[8]D. Chapman *et al.*, Phys. Plasmas **21**, 082709 (2014).
[9]D. Kraus *et al.*, Phys. Rev. E **94**, 011202(R) (2016).
[10]B. Beckhoff *et al.*, Proc. SPIE **2859**, 190 (1996).
[11]T. Döppner *et al.*, Rev. Sci. Instrum. **79**, 10E311 (2008).
[12]B. R. Maddox *et al.*, Rev. Sci. Instrum. **82**, 023111 (2011).